Calibration and Uncertainty Evaluation Using Monte Carlo Method of a Simple 2D Sound Localization System

Luigi Battista, Emiliano Schena, *Member, IEEE*, Giuseppina Schiavone, Salvatore Andrea Sciuto, and Sergio Silvestri, *Member, IEEE*

***Abstract*— A simple measurement system (MS) is developed to perform sound localization on a plane and evaluate its performances with specific attention to calibration and uncertainty evaluation. The sensing element is composed of two microphones mounted at the left and right ears on a cap. The localization of sound source is obtained by the estimation of the delay between the time instants of arrival of the sound to the two microphones, through a cross-correlation technique. The principle of this paper is described in mathematical terms and is experimentally validated in the azimuthal angle (θ) range $\pm$ 90° at three different distances between the microphones. The MS has a nonlinear response over the whole range, on the other hand it can be considered linear within $\pm$ 15°. In addition, the sensor presents a low discrimination threshold (2°). The uncertainty evaluation of the MS is performed using the propagation of uncertainty and the Monte Carlo method: simulations show an uncertainty < ∼5° in the range $\pm$ 90°. The characteristic of wearability, typical feature of sensors used to perform early detection of disorders, the good accuracy and resolution allow the chance to introduce the MS in the field of developmental psychology and, in particular, as a support for early diagnosis of pervasive developmental disorders (e.g., autism spectrum disorders).**

***Index Terms*— Monte Carlo method, sound localization, uncertainty evaluation, sound localization sensors.**

I. Introduction

SOUND localization is essential in several fields including video conferencing and surveillance, and it represents a fundamental function for robots interacting with humans [1]. The localization of a sound source is mostly based on steerable beam-forming and on time delay estimation obtained from the data processing of two or more signals picked up by different microphones.

L. Battista and S. A. Sciuto are with the Department of Mechanical and Industrial Engineering, Roma Tre University, Rome 00154, Italy (e-mail: luigi.battista@uniroma3.it; salvatore.sciuto@uniroma3.it).

E. Schena and S. Silvestri are with the Center for Integrated Research, Unit of Measurements and Biomedical Instrumentation, Università Campus Bio-Medico di Roma, Rome 00128, Italy (e-mail: s.silvestri@unicampus.it; e.schena@unicampus.it).

G. Schiavone is with the Advanced Concepts Team, European Space Research & Technology Centre, Noordwijk 2200 AG, The Netherlands (e-mail: giusy.schiavone@gmail.com).

Color versions of one or more of the figures in this paper are available online at http://ieeexplore.ieee.org.

.

In order to localize a sound source in 3D space, three or more pressure sensors [2] are needed [3]; whereas, only two microphones are adequate to localize sound source on a plane.

The MS reported here, is able to localize a sound source if both the microphones and the sound source belong to the same azimuthal plane [4]. The theory of operation for sound source localization on a plane is based on the calculation of the time delay of arrival (TDOA) between the two microphones. This is a biomimetic approach: the time difference between the time of arrival of a sound to ears, the interaural time difference (ITD), is used by humans and animals to localize sound sources. Recently, researchers have developed measurement systems based on dynamic information in order to improve the accuracy [5].

In this paper we present the principle of measurement, the realization and the static calibration of a simple sound source MS. We focused our attention on the evaluation of its accuracy, because, in literature, we did not find a full investigation about the uncertainty associated to this kind of MS. The sensing element is composed of two microphones mounted on a cap at the left and right ears; this arrangement allows to perform measurements in unstructured environment. The good accuracy and resolution, see sections IV and V, offer the chance to introduce the MS in the field of developmental psychology [6]. It could be used as a support for early diagnosis of pervasive developmental disorders, such as Autism spectrum disorders (ASD). Diagnostic trials for ASD are not available in literature and therefore the diagnosis is merely clinical. However, during the last decade, different studies were conducted to diagnose ASD through the analysis of motor domain impairment in children [7], [8]. The MS should be used to assess sensory integration in social orienting behavior in children: the sensor tracks child's head orientation when he is acoustically stimulated by a human operator sitting in front of him focusing on altered responses to sound stimuli [9].

The localization of sound source on a plane is carried out by an estimation of ITD through a cross-correlation technique: it is necessary to outline that some methods to reduce the effects due to reverberation have been proposed (e.g., a method based on the generalized cross correlation [10] and a method exploiting the knowledge of geometrical relationships of the sensors in obtaining the time delay [11]). However the reported measurement technique allows a maximum accuracy

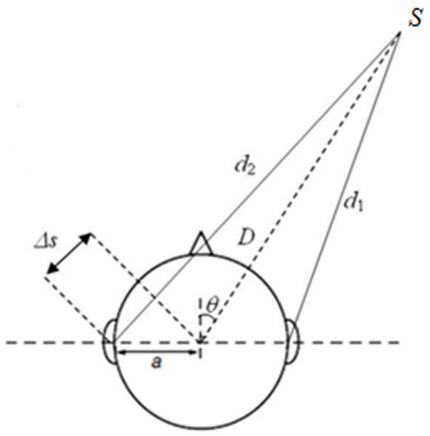

Fig. 1. Geometrical–based model to calculate ITD.

in the estimation of sound source direction of about 5°; the accuracy of the simple MS reported here is quite similar (see Section V). The static calibration is performed under two different conditions (in absence or in presence of the head between the two microphones) and using three different distances between the two microphones. A comparison between two commonly used mathematical models is also carried out [12].

The performances of sound localization methods have been analyzed by some researchers with different techniques (e.g., improvement of beam forming method and the use of complexity measurements, like with Permutation Entropy) [3], [5], [13]–[15]. However, the influence of main physical quantities on system uncertainty, such as air environmental temperature and distance between two microphones, were not considered. In this work, the uncertainty has been evaluated with two different approaches: the law of propagation of uncertainty [16] and the MCM [17]. The influence of distance between the two microphones, environmental temperature, and acquisition frequency of the signal received by the microphones on the uncertainty have also been assessed.

II. Operation Principle

The sensing element is composed of two omni-directional microphones nominally positioned in correspondence of the subject ears (Fig. 1). The localization of the sound source (S) is based on the evaluation of the time difference between the times of arrival of the sound wave to the microphones, i.e., ITD, due to the different path length of the sound wave. With reference to Fig. 1, the head radius has been indicated with a, the distance of S from the head center with D, d_1 and d_2 are the distances between S and respectively right and left microphones, Δs is the path difference, and θ is the azimuthal angle which has to be estimated. If $\theta = 0°$, the distances covered by a sound wave to reach the two microphones are equal, and this results into ITD = 0; if $\theta \neq 0°$, the distances are different, therefore ITD $\neq$ 0, and it reaches the maximum value for $\theta = 90°$.

The ITD value depends on several factors [18]: mainly θ, the interaural distance (2a), the sound wave frequency (f), the speed of sound in the air (c). In this paper, two geometrical simplified approaches are presented in order to calculate the ITD, depending on the absence or presence of the head between the microphones.

The first approach describes the MS without the head between the two microphones (Fig. 1); under the hypothesis of propagation of plane sound wave in free field conditions, and consequently under the assumptions $d_2 \approx D+\Delta s$ and $d_1 \approx D-\Delta s$, the following relationship can be geometrically derived:

$$ITD = \frac{d_2 - d_1}{c} \cong \frac{(D + \Delta s) - (D - \Delta s)}{c} = 2\frac{\Delta s}{c} = \frac{2 \cdot a}{c} \sin(\theta) \quad (1)$$

where ITD is independent of frequency f under the previously stated assumptions.

The second approach (Fig. 1) takes into account the presence of a spherical head between the microphones [12] and it refers to the propagation of a sound plane wave in free field condition and to the diffraction of an harmonic plane wave by the head which is assumed to be spherical [19]:

$$ITD \cong \frac{a}{c}[\theta + \sin(\theta)] \quad (2)$$

where ITD is independent of frequency f under the previously stated assumptions [19].

For small θ, we may consider$\sin(\theta) \cong \theta$; this hypothesis causes a maximum approximation equal to about 1% for θ in the range $\pm$ 15°, and we obtain the following linear model by (1) and (2):

$$ITD \cong \frac{2 \cdot a}{c}\theta \quad (3)$$

The microphone signals are processed in order to estimate the ITD value. The processing algorithm plays a key role in the correct evaluation of the ITD. In order to use a robust algorithm, we have estimated the ITD by means of cross-correlation between the signals received by the microphones: the instant corresponding to the maximum of the cross-correlation curve represents the ITD value [20]:

$$ITD = \arg\max(m_l \otimes m_r) = \arg\max\left(\int_{-\infty}^{\infty} m_l^*(\tau) \cdot m_l^*(t+\tau)\, d\tau\right) \quad (4)$$

where $m_l(t)$ and $m_r(t)$ are the signals picked up by left and right microphones respectively.

As the ITD has been obtained, θ can be calculated either by (1) and (2) or by the linear model (3).

III. Experimental Setup and Measurement System Simulations

Experimental trials were carried out in order to calibrate the MS and to verify the mathematical model (1–3).

Sound waves, produced by a magnetic transducer buzzer (EMX-300) characterized by a fundamental frequency of about 460 Hz, reach the omni-directional microphones (Sennheiser MKE-2 EW-3 Gold) fixed on two vertical bars, or onto a sphere, mounted on a rotating platform. The distance between

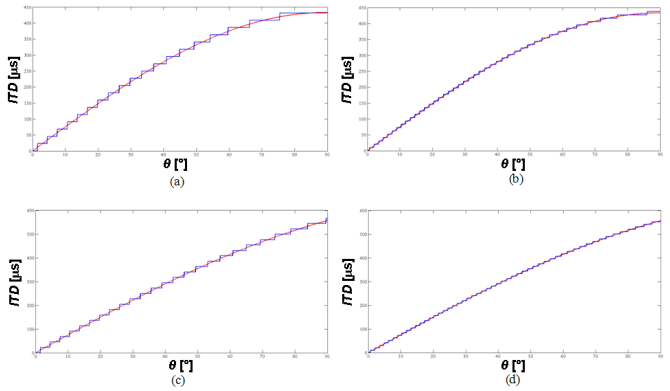

Fig. 2. Theoretical model (continuous curve) and resolution (discontinuous curve) of the MS output vs θ for 2a = 150 mm. (a) f_s = 44100 Hz, without head (1); (b) f_s = 96000 Hz, without head (1); (c) f_s = 44100 Hz, with head (2); (d) f_s = 96000 Hz, with head (2).

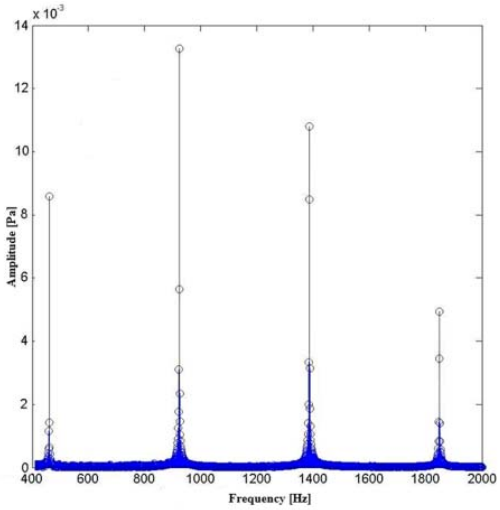

Fig. 3. Frequency spectrum of the signal picked up by one of the two microphones when the buzzer EMX-300 was tested. The measured sound pressure level at the microphone is of about 40 dB.

the two bars, or the sphere diameter, represents 2a. It is possible to set different distances between the vertical bars or use spheres with different diameters in order to evaluate the influence of 2a on the calibration curve. The rotating platform shows a rotational scale with 1° resolution allowing to set different θ in the range ± 90°. The buzzer, mounted on a vertical bar, is placed at the same height of the microphones, therefore, it belongs to the azimuthal plane. Sound signals, received by the microphones, are picked up by a sound card (TASCAM- US-144) by means of a pre-amplifier (Sennheiser MZA 900 P), are digitized and sent to a PC. The sound card allows to acquire data at different sampling frequencies (800 Hz, 1600 Hz, 22050 Hz, 44100 Hz, 48000 Hz, 96000 Hz). Signal sequences, with duration of 200 ms, are cut into 100 subsequences with duration of 2 ms. Data are then processed in MATLAB environment. Cross-correlation is performed between each pair of the abovementioned 100 subsequences. The maximum value obtained from each of the 100 cross-correlations corresponds to a specific time delay, calculated by (4): an estimation of ITD is derived from the time delay that most frequently occurs, if the correspondent relative frequency is greater than 0.70. In fact, the 100 cross-correlations were expected to assume the maximum value for the same time delay for the time resolution of the sound card (for a sampling frequency fs of 96000 Hz, time resolution, Ts, is 1/fs≈10 μs).

Hundred cross-correlations were carried out in order to perform an estimation of ITD by considering a large number of samples, so that statistical significance is get better, and consequently in order to obtain the rejection of incorrect values of delay due to noise, or reflections and diffractions of the sound waves.

Since the theoretical resolution of the MS is limited by fs, simulations were carried out in order to evaluate the influence of fs on the resolution of MS: the sensor is not able to discriminate two ITDs with a difference shorter than Ts/2. Equation (1) and (2) are used to simulate ITD as a function of θ, with c = 340 m/s, 2a = 150 mm, and two different sampling frequencies, 44100 Hz and 96000 Hz, as shown in Fig. 2.

As expected, simulations show that the theoretical resolution decreases with θ and if fs decreases. In fact, using (1) the following results were obtained: with fs = 96000 Hz for $\theta < 15°$ the theoretical resolution is 2°, and for $\theta > 75°$ is 9°; with fs = 44100 Hz for $\theta < 15°$ the theoretical resolution is 4°, and for $\theta > 75°$ is 15°. The resolution is better when the presence of the head is taken into account (2): with fs = 96000 Hz for $\theta < 15°$ the theoretical resolution is 1°, and for $\theta > 75°$ is 3°; with fs = 44100 Hz for $\theta < 15°$ the theoretical resolution is 3°, and for $\theta > 75°$ is 6°. Moreover, the simulations show that the microphone signals must be sampled setting fs equal to 96000 Hz in order to maximize the resolution of MS.

The experimental set up allowed us to calibrate the sensor in the range ± 90°, in steps of 15° set through the rotating platform. According to the increase of the theoretical resolution and in order to validate the linear model (3), in the range ± 15° the angle interval was reduced and a high number of angles was tested. In the following all results are reported as the measured ITD ± 5 μs. The uncertainty (5 μs) was considered equal to Ts/2, representing one-half of the MS resolution in the discrimination of two different ITD.

IV. Experimental Results and Discussion

Preliminary trials were carried out in order to assess the frequency characteristics of the sound waves emitted by the buzzer. A power supply unit (DC ISO-TECH IPS2302A) was used to power the buzzer (Val = 5.00 ± 0.01 V); a microphone (Sennheiser MKE 2-EW-3 Gold, flat frequency response up to 20 kHz) was used to sense the wave sound. The frequency spectrum of the signal, processed in MATLAB environment, is presented in Fig. 3.

The first harmonic of the sound wave, placed at 462 Hz, is within the bandwidth of the microphones. The ambiguity condition can be expressed by the following equation:

$$ITD = \frac{a}{c}(\sin\theta+\theta) \leq \frac{T}{2} \Rightarrow f \leq \frac{1}{2 \cdot \frac{a}{c}(\sin\theta+\theta)} = f_c \quad (5)$$

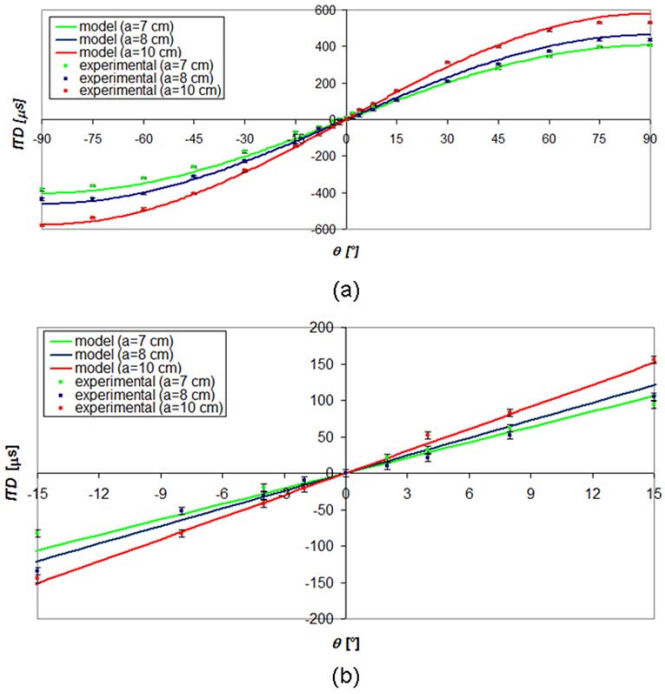

Fig. 4. Comparison between the theoretical model and the experimental data obtained from the calibration using three different interaural distances: green (140 mm), blue (160 mm), red (200 mm). (a) Mathematical model (1); (b) linear model (3).

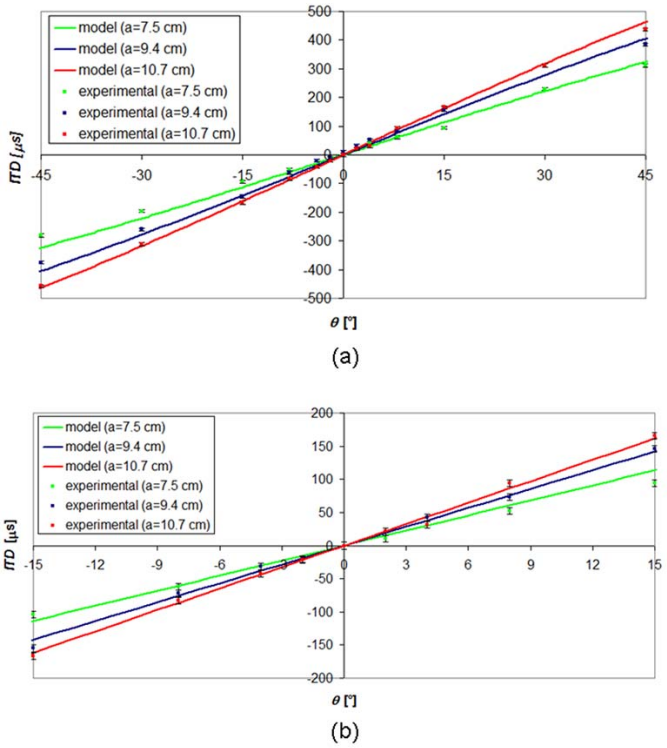

Fig. 5. Experimental data obtained from calibration using three spheres with different interaural distance: green (150 mm), blue (188 mm), red (214 mm). (a) Mathematical model (2); (b) linear model (3).

where fc is the threshold frequency value: when the sound wave presents the fundamental harmonic frequency lower than fc, the ambiguity is avoided. The buzzer allows to avoid the ambiguity in overall range of calibration; in fact, for θ in the range $\pm$ 90° and considering the values of 2a used in the calibration (ranging between 140 mm and 200 mm), the ambiguity occurs at a frequency value (about 800 Hz) greater than 462 Hz. As the first harmonic presents a frequency value within the human hearing range and it does not present ambiguity in the range of 2a including typical values for children [21], this buzzer should be used as the acoustic stimulus placed in front of the child.

Three sets of measurements were performed for static calibration without the head between the two microphones: three different values of 2a (140 mm, 160 mm, 200 mm) were set in order to evaluate the influence on the calibration curve. The experimental ITD values and the mathematical model (1) as a function of θ, for different 2a are reported in Fig. 4(a). Fig. 4(b) shows the experimental data and the linear mathematical model (3) between $-15°$ and $15°$.

Fig. 4 shows that experimental data agree with the theoretical model ($r^2 > 0.96$). Experimental results in the range $\pm$ 15° show a good fitting with linear model (3): $r^2 = 0.964$ for $2a = 140$ mm, $r^2 = 0.973$ for $2a = 160$ mm and $r^2 = 0.997$ for $2a = 200$ mm. They also show that the MS sensitivity increases with 2a (e.g., in the linear range sensitivity is about 6 μs/° for $2a = 140$ mm, 7 μs/° for $2a = 160$ mm and 10 μs/° for $2a = 200$ mm). The MS resolution is better than 4° for small θ and gets worse for θ near to $|90°|$ (in fact the sensor does not resolve θ between 75° and 90°), as shown by simulations (Fig. 2(a) and 2(c)). A further valuable characteristic is related to the discrimination threshold (2°).

Three sets of experimental trials were carried out for static calibration with the head, simulated by a polymeric sphere filled with water placed between the microphones: three spheres with different diameters (150 mm, 188 mm, 214 mm) were used. The different above mentioned values of interaural distance have been chosen according to typical anthropometric data of the head circumference [21].

Fig. 5(a) and Fig. 5(b) show the experimental data and the mathematical models (2) and (3).

Fig. 5 shows a good agreement between experimental data and the theoretical model (3), $r^2 > 0.98$. Experimental results for θ in the range $\pm$ 15° show a good fitting with linear model (3): $r^2 > 0.980$ in all trials. They also show that MS sensitivity increases with 2a (e.g., in the linear range sensitivity is 6 μs/° for $2a = 150$ mm, 9 μs/° for $2a = 188$ mm and 11 μs/° for $2a = 214$ mm). Experimental trials were carried out with θ in the range $\pm$ 45° because the diffraction of sound waves on the head makes the MS not able to measure the ITD for θ higher than 45° [12]. The MS resolution is confirmed to be better than 4° for small θ in accordance with the simulations (Fig. 2d) and the minimum detectable angle variation is < 2°.

The above quoted agreement, the good resolution and the accuracy (as detailed in the following Section) allow to introduce the MS for sound socalization in the field of developmental psychology, in particular for supporting early diagnosis of the Autism spectrum disorders (ASD). In fact,

the MS should be used to assess sensory integration in social orienting behavior in children; the sensor tracks child's head orientation when he is acoustically stimulated by a human operator sitting in front of him focusing on altered responses to sound stimuli [9].

V. Evaluation of Uncertainty

There are no previous study in the literature, in which a full investigation about the uncertainty associated to this kind of MS was performed; some studies [22] proposed only methods for the analysis of the front-back confusion (i.e., a condition verified when ITD can be mapped to multiple regions in plane). As θ cannot be directly measured, the influence of the three physical quantities (i.e., 2a, ITD, and c) of the model (1–3) on the MS uncertainty has been estimated. This evaluation has been carried out in the whole range of calibration using two different approaches: 1) propagation of uncertainty [16]; 2) propagation of distributions using MCM [17].

The first step was the definition of a measurement model expressing the measurand as a function of the input quantities (ITD, c, 2a). The model used is described by (2), taking into account the presence of the head. The dependence of c with the environmental temperature can be expressed by the following empirical equation:

$$c\,(t) = c_0\sqrt{1+\frac{t}{T_0}} \tag{6}$$

where c_0 is the sound speed in air at 0 °C (331.3 m/s), T_0 is equal to 273.15 °C and t is the temperature of the air [23].

Introducing (6) in (2) and making explicit θ using the Padè approximant [24]:

$$\theta = -\frac{2\cdot\left(-6+\sqrt{36-3\cdot\left(\frac{ITD\cdot c_0\sqrt{1+\frac{t}{T_0}}}{a}\right)^2}\right)}{\frac{ITD\cdot c_0\sqrt{1+\frac{t}{T_0}}}{a}} \tag{7}$$

The second step was the assignment of probability density functions (PDFs) to input quantities. A gaussian PDF ($2\bar{a}$ = 151 mm, σa = 14 mm) was assigned to 2a. The mean and standard deviation values were obtained from anthropometric studies on the head circumference [21]. A gaussian PDF ($\bar{t} = 22\ ^\circ C$, $\sigma_t = 2\ ^\circ C$) was assigned to t, hypothesizing that the measurements are carried out in-house where t is controlled. As ITD was measured as described in section 3, the only available information is that ITD can present a difference from the measured value lower than $T_S/2$. Therefore a rectangular PDF was assigned to ITD (mean equal to the ITD value measured and width equal to the sampling period, 10 μs) was chosen, as recommended in [14].

The propagation of uncertainty, under the hypothesis of uncorrelated input quantities, was implemented by the following equation:

$$\delta\theta = \sqrt{\left(\frac{\partial\theta}{\partial ITD}\delta ITD\right)^2+\left(\frac{\partial\theta}{\partial a}\delta a\right)^2+\left(\frac{\partial\theta}{\partial t}\delta t\right)^2} \tag{8}$$

TABLE I
Uncertainty Values of Θ Evaluated Through the Two Approaches Considering Different PDFs

	PDFs used in the first case (poor knowledge of the input quantities)			*PDFs used in the second case (2a and t were measured)*		
ITD [µs]	θ [°]	$\delta\theta$ [°] (8) (95%)	$\delta\theta$ [°] MCM (95%)	θ [°]	$\delta\theta$ [°] (8) (95%)	$\delta\theta$ [°] MCM (95%)
0	0.0	0.7	0.7	0.0	0.7	0.6
10	1.4	0.8	0.7	1.4	0.7	0.6
31	4.1	1.0	1.0	4.0	0.7	0.7
63	8.3	1.7	1.7	8.2	0.7	0.8
115	15.2	3.1	2.9	15.1	0.8	0.9
219	29.5	6.3	5.7	29.2	1.2	1.4
323	44.8	9.9	9.2	44.3	1.8	2.0
417	60	14	13	59.4	2.4	2.7
490	74	20	18	74.7	3.3	3.5
552	88	26	25	88.0	4.3	4.5

The uncertainty of the input quantities was evaluated considering a confidence level of 95%. The propagation of PDFs was implemented through the MCM selecting a number of trials m equal to 10^6. Table 1 shows the results obtained by the two approaches with a confidence level of 95%.

Table 1 shows that the measurement uncertainty increases with θ (e.g., for $\theta > 45^\circ$ the uncertainty is greater than 9.2°). The results obtained by MCM (Fig. 6(a)) and by the propagation of uncertainty (8) are similar (table 1), and in particular, MCM gives an uncertainty lower than uncertainty propagation in for θ wider than 45°, these results are caused by the non-linearity of the model.

The relatively high uncertainty values depend on the poor knowledge of the input quantities (in particular for 2a and t) showing high standard deviation values.

The measurement uncertainty can be minimized by improving the knowledge of the input quantities: an accurate measurement of the input quantities allows to reduce the PDFs standard deviations and this causes a decrease of θ uncertainty. As an example, a scenario where the 2a and t were obtained by measuring instruments was considered. Thanks to this hypothesis was assigned the following PDFs: a rectangular PDF for 2a with a mean equal to a typical value for infants (151 mm) and width equal to 10 mm (this uncertainty can be easily obtained by using a tape measurement), a gaussian PDF for the environmental temperature with mean of 22.0 °C and standard deviation of 0.3 °C (this uncertainty can be easily obtained through a cost effective sensor of temperature), and a rectangular PDF for ITD with width of 10 μs.

The uncertainty was calculated through the steps described above. The results are also reported in Table 1 and the PDFs of θ obtained by MCM are shown in Fig. 6(b).

Table 1 shows that the uncertainty is < 5° in the whole range of calibration and increases with θ, while the uncertainties calculated through the two different approaches are very similar. A comparison of the results reported in Table 1, using different PDFs, shows the improvement of measurement results obtained by means of a knowledge of the input quan-

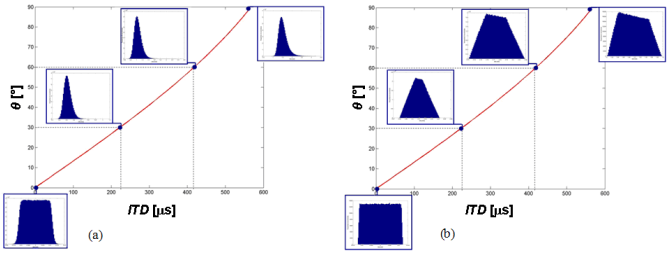

Fig. 6. Mathematical model expressed by (7) and the PDFs of θ obtained assigned different PDFs to the input quantities: (a) the PDFs of input quantities without further measurements, (b) with measurement of 2a and t.

tities obtained by further measurements, e.g., the uncertainty decreases from 26° to 4.5° at the full scale, from 9.2° to 2.0° in the middle of measurement range and from 3° to 0.8° for θ equal to about 15° .

Fig. 6 shows that the PDFs of θ loses symmetry when θ increases due to the non-linearity of the model. It also shows the different shape of the PDFs, obtained introducing different PDFs for the quantities in the model.

VI. Conclusion

In conclusion, a sound localization sensor has been realized and calibrated. The measurement principle is based on the estimation of ITD through a cross-correlation of two signals picked up by two microphones placed in binaural configuration and mounted on a cap; the experimental data of static calibration are in accordance with the mathematical model (based on the assumption of sound plane wave propagating in free field condition) and with the simulations of the theoretical resolution.

An in-depth study of the measurement uncertainty has also been performed considering two scenarios, respectively with a poor knowledge of the input quantities and with an accurate knowledge of them. The former, based on an estimation of the interaural distance PDF through anthropometric data and of the air temperature PDF according to work conditions, presents a maximum value, in the whole range of calibration, of $\delta\theta = 24°$, obtained with MCM; considering the scenario where the input quantities (2a and t) are measured, a maximum value of $\delta\theta = 4.5°$ in the whole range of calibration, is obtained: a more accurate measurement of the input quantities allows to reduce considerably the uncertainty of θ, as expected for nonlinear systems.

The good accuracy and resolution allow to introduce the MS in the field of developmental psychology, in particular for supporting early diagnosis of the Autism spectrum disorders (ASD).

Furthermore, the improvement of the device accuracy can also be crucial for some applications, such as sound localization system of mobile robots interacting with humans and on surveillance equipment, development of sound localization system for deaf people, researches investigating the complex mechanism of human hearing, in fact several structures in auditory system respond to the cues in order to perform sound localization.

References

[1] Y. Rui, D. Florencio, W. Lam, and J. Su, "Sound source localization for circular arrays of directional microphones," in *Proc. IEEE Int. Conf. Acoust., Speech, Signal Process.*, vol. 3. Mar. 2005, pp. 93–96.

[2] M. Cannella, P. Cappa, and S. A. Sciuto, "A novel approach for determining the trajectory and speed of a supersonic object," *Meas. Sci. Technol.*, vol. 14, no. 5, pp. 654–662, May 2003.

[3] J. Huang, N. Ohnishi, and N. Sugie, "Spatial localization of sound sources: Azimuth and elevation estimation," in *Proc. IEEE Int. Conf. Instrum. Meas. Technol. Conf.*, vol. 1. May 1998, pp. 330–333.

[4] A. A. Handzel and P. S. Krishnaprasad, "Biomimetic sound-source localization," *IEEE Sensors J.*, vol. 2, no. 6, pp. 607–616, Dec. 2002.

[5] I. Toshima and S. Aoki, "Sound localization during head movement using an acoustical telepresence robot: TeleHead," *Adv. Robot.*, vol. 23, no. 3, pp. 289–304, 2009.

[6] S. Patel, H. Park, P. Bonato, L. Chan, and M. Rodgers, "A review of wearable sensors and systems with application in rehabilitation," *J. Neuroeng. Rehabil.*, vol. 9, no. 1, pp. 21–38, Apr. 2012.

[7] G. Schiavone, D. Formica, F. Taffoni, D. Campolo, E. Guglielmelli, and F. Keller, "Multimodal ecological technology: From child's social behavior assessment to child-robot interaction improvement," *Int. J. Soc. Robot.*, vol. 3, no. 1, pp. 1–13, Jan. 2010.

[8] J. Pinto-Martin and S. E. Levy, "Early diagnosis of autism spectrum disorders," *Current Treatment Opt. Neurol.*, vol. 6, no. 5, pp. 391–400, Oct. 2004.

[9] A. T.-S. Wolfgang, K. L. Pierce, E. Courchesne, and S. A. Hillyard, "Auditory spatial localization and attention deficits in autistic adults," *Cognit. Brain Res.*, vol. 23, nos. 2–3, pp. 221–234, May 2005.

[10] C. H. Knapp and G. C. Carter, "The generalized correlation method for estimation of time delay," *IEEE Trans. Acoust. Speech, Signal Process.*, vol. ASSP-24, no. 4, pp. 320–327, Aug. 1976.

[11] H. Atmoko, D. C. Tan, G. Y. Tian, and B. Fazenda, "Accurate sound source localization in a reverberant environment using multiple acoustic sensors," *Meas. Sci. Technol.*, vol. 19, no. 2, p. 024003, Feb. 2008.

[12] G. Kuhn, "Model for interaural time differences in the azimuthal plane," *J. Acoust. Soc. Amer.*, vol. 62, no. 1, pp. 157–167, 1977.

[13] A. Lay-Ekuakille, P. Vergallo, D. Saracino, and A. Trotta, "Optimizing and post processing of a smart beamformer for obstacle retrieval," *IEEE Sensors J.*, vol. 12, no. 5, pp. 1294–1299, May 2012.

[14] P. Vergallo, A. Lay-Ekuakille, N. I. Giannoccaro, A. Massaro, S. Urooj, D. Caratelli, and A. Trabacca, "Processing EEG signals through Beamforming techniques for seizure diagnosis," in *Proc. 6th Int. Conf. Sens. Technol.*, Dec. 2012, pp. 497–501.

[15] F. C. Morabito, D. Labate, F. La Foresta, A. Bramanti, G. Morabito, and I. Palamara, "Multivariate multi-scale permutation entropy for complexity analysis of alzheimer's disease EEG," *Entropy*, vol. 14, no. 7, pp. 1186–1202, Jul. 2012.

[16] *Evaluation of Measurement Data—Guide to the Expression of Uncertainty in Measurement*, JCGM, London, U.K., 2008.

[17] *Evaluation of Measurement Data—Supplement 1 to the Guide to the Expression of Uncertainty in Measurement—Propagation of Distributions Using a Monte Carlo Method*, JCGM, London, U.K., 2008.

[18] D. Wang and G. J. Brown, *Computational Auditory Scene Analysis: Principles, Algorithms and Applications*. New York, NY, USA: Wiley, 2006.

[19] R. S. Woodworth and H. Schlosberg, *Experimental Psychology*. New York, NY, USA: Holt, Rinehart and Winston, 1962.

[20] J. Blauert, *Spatial Hearing: The Psychophysics of Human Sound Localization*. Cambridge, MA, USA: MIT Press, 1997.

[21] A. F. Roche, D. Mukherjee, S. Guo, and W. M. Moore, "Head circumference reference data: Birth to 18 years," *Pediatrics*, vol. 79, no. 5, pp. 706–712, May 1987.

[22] Y. Park, S. Hwang, and J. Park, "A probabilistic method for analysis of sound localization performance," *Appl. Acoust.*, vol. 70, no. 5, pp. 771–776, May 2009.

[23] G. S. K. Wong and T. F. W. Embleton, "Variation of the speed of sound in air with humidity and temperature," *J. Acoust. Soc. Amer.*, vol. 77, no. 5, pp. 1710–1712, Jan. 1985.

[24] H. Padè, "Sur la representation aprochee d'une fonction par des fractions rationnelles," *Annales Scientifiques École Normale Supérieure*, vol. 9, no. 3, pp. 3–93, 1892.

Luigi Battista received the Ph.D. degree in engineering from the University of Rome "Roma Tre," Rome, Italy, in 2013. His current research interests include biomedical instrumentation and fiber-optic sensors for mechanical and thermal measurements.

Emiliano Schena (M'10) received the Ph.D. degree in biomedical engineering from the University Campus Bio-Medico of Rome, Rome, Italy, in 2009. His current research interests include sensors and transducers for mechanical and thermal measurements applied to biomedical devices and instrumentation, fiber optic-based measurement systems, and respiratory rehabilitation.

Giuseppina Schiavone received the Ph.D. degree in biomedical engineering from the University Campus Bio-Medico of Rome, Rome, Italy, in 2010. His current research interests include the design of system to perform early diagnosis of pervasive developmental disorders.

Salvatore Andrea Sciuto is currently a Professor of measurements and biomedical instrumentation with the University Roma TRE, Rome, Italy. His current research interests include sensors for biomedical devices and instrumentation, neonatal artificial ventilation, and non-invasive medical measurements.

Sergio Silvestri received the Ph.D. degree in mechanical and thermal measurements from Cagliari University, Cagliari, Italy, in 2001, and is currently an Associate Professor of measurements and biomedical instrumentation with the University Campus Bio-Medico of Rome, Rome, Italy. His current research interests include sensors for biomedical devices and instrumentation, neonatal artificial ventilation, and non-invasive medical measurements.